PRE-FILTERING FOR CLUTTER REJECTION IN BEAMSPACE STAP

Mehdi Khanpour-Ardestani, Dept. of Elec. and Comp. Eng., University of Toronto
Raviraj S. Adve, Ph. D., Dept. of Elec. and Comp. Eng., University of Toronto
Michael C. Wicks, Ph.D., Sensors Directorate, US Air Force Research Laboratory

Key Words: Space-Time Adaptive Processing, Pre-filtering, Clutter Rejection.

ABSTRACT

Several space-time adaptive processing algorithms have been proposed to detect weak targets in the presence of strong interference, especially clutter and jamming. Except for Displaced Phase Center Array (DPCA) processing, radar signal processing algorithms ignore the fact that the location of the clutter ridge in angle-Doppler space is known, given the platform speed and direction. This paper introduces our attempt to exploit this *a priori* knowledge in conjunction with the joint domain localized processing algorithm. Using a two-dimensional filter, clutter is rejected in a first, non-adaptive stage, followed by adaptive processing in the angle-Doppler domain.

1. *INTRODUCTION*

Airborne surveillance radar systems operate in a severe and dynamic interference environment. Space-Time Adaptive Processing (STAP) techniques promise to be the best means to detect weak targets in such interference. STAP algorithms process data in two dimensions, separating the target from interference in both angle and Doppler. Consider a phased array antenna with N spatial channels, and M pulses per Coherent Processing Interval (CPI). The most straightforward STAP algorithm uses all NM degrees of freedom (DOF), estimating the NM dimensional covariance matrix of the interference to minimize the expected squared error with respect to the desired signal [1]. It is now well accepted that this fully adaptive algorithm is impractical, since it is impossible to obtain enough data samples to estimate such a large covariance matrix, and the associated computation load is prohibitive.

To overcome the drawbacks of the fully adaptive algorithm, researchers have proposed several algorithms that limit the number of adaptive weights [2]. In particular, Wang and Cai introduced the Joint Domain Localized (JDL) algorithm, a popular post-Doppler, beam-space approach that adaptively processes radar data after transformation to the angle-Doppler domain [3]. Processing is restricted to a Localized Processing Region (LPR) in the transform domain, significantly reducing the number of DOF, while retaining maximal gain against thermal noise. The reduced DOF leads to corresponding reductions in required sample support and computation load.

In airborne radar, one crucial, indeed often dominant, component of the interference is the ground clutter. Due to the motion of the radar platform, the clutter occupies a *clutter ridge* in the angle-Doppler domain, i.e., after transforming the space-time data to the angle-Doppler domain, the clutter is localized along a line [2]. The slope of this line is determined by the speed of the airborne platform, a parameter that may reasonably be assumed known. *The location of the clutter in angle-Doppler space is therefore known a-priori*. This information has been used in non-adaptive processing, most commonly by DPCA processing, however *has been ignored in the development of STAP algorithms*.

A central question asked in this paper is how to exploit this *a priori* information. This work develops a simple extension of the JDL algorithm that uses knowledge of the location of the clutter ridge to pre-filter the clutter. The resulting space-time signal is then processed to detect weak targets. A crucial factor in the success of this algorithm is the ability to model the changes in the space-time steering vector. The model for the change in the space-time steering vector was developed in [4]. With minimal increase in computation load, the pre-filtering approach results in significant performance gains.

This paper is organized as follows. Section 2 briefly reviews the JDL algorithm as modified in [3] and then introduces the pre-filtering technique developed here. Section 3 presents numerical examples, using both simulated and measured data, to illustrate the performance improvements to be had by using pre-filtering. Section 4 ends the paper with a summary and some conclusions.

2. *CLUTTER PRE-FILTERING*

We begin with a brief summary of the JDL algorithm as developed in [4]. In the JDL algorithm, target and interference are transformed to η_a angle and η_d Doppler bins forming an $\eta_a \times \eta_d$ LPR. This is achieved using a transformation matrix comprising the space-time steering vectors corresponding to the angle-Doppler bins in the LPR. Representing as $\mathbf{a}(\theta)$ the length-N spatial steering vector associated with angle θ and $\mathbf{b}(f_d)$ as the length-M temporal steering vector corresponding to Doppler frequency f_d, the transformation matrix $\mathbf{T}$ for $\eta_a = \eta_d = 3$, is given by

$$\mathbf{T} = \left[\mathbf{b}(f_{-1})\ \ \mathbf{b}(f_0)\ \mathbf{b}(f_1)\right]_{M\times 3} \otimes \left[\mathbf{a}(\theta_{-1})\ \mathbf{a}(\theta_0)\ \ \mathbf{a}(\theta_1)\right]_{N\times 3} \quad (1)$$

$$= \left[\mathbf{s}(f_{-1},\theta_{-1})\ \ \mathbf{s}(f_{-1},\theta_0)\ \mathbf{s}(f_{-1},\theta_1)\ \mathbf{s}(f_0,\theta_{-1})\right.$$
$$\left.\mathbf{s}(f_0,\theta_0)\ \mathbf{s}(f_0,\theta_1)\ \ \mathbf{s}(f_1,\theta_{-1})\ \ \mathbf{s}(f_1,\theta_0)\ \ \mathbf{s}(f_1,\theta_1)\ \right], \quad (2)$$

where the LPR encompasses angles θ_{-1}, θ_0 and θ_1 and Doppler frequencies f_{-1}, f_0 and f_1 and $\mathbf{s}(f_d, \theta) = \mathbf{b}(f_d) \otimes \mathbf{a}(\theta)$ represents the length-*NM* space-time steering vector.

The transform domain data *and transform domain steering vector* are given by

$$\tilde{\mathbf{x}} = \mathbf{T}^H \mathbf{x}, \quad (3)$$

$$\tilde{\mathbf{s}} = \mathbf{T}^H \mathbf{s}. \quad (4)$$

$$\tilde{\mathbf{w}} = \tilde{\mathbf{R}}^{-1} \tilde{\mathbf{s}}, \quad (5)$$

where the tilde (˜) represents the transform domain, **x** represents the length-*NM* space-time data vector and **s** the length-*NM* target steering vector. $\tilde{\mathbf{x}}$ represents the length-$\eta_a\eta_d$ vector of data within the LPR and $\tilde{\mathbf{w}}$ the length-$\eta_a\eta_d$ adaptive weight vector in the transform domain. The matrix $\tilde{\mathbf{R}}$ represents the estimated covariance matrix in the transform domain.

In this work, the space-time data is first filtered using a *two dimensional* band-stop finite impulse response (FIR) filter. The stop band of this filter is chosen to match the location of the clutter ridge, i.e., the filter rejects the clutter and allows all other signals through. The filter is designed using frequency sampling [4]. The design process requires identification of the filter response at a finite number of points in angle-Doppler space. The frequency response of the resulting FIR filter is then guaranteed to equal the desired response at these points in angle-Doppler space. The process and results in a matrix, **W**, of filter coefficients.

Later in this paper we present results using simulated data wherein the clutter ridge has unit slope in the spatial-frequency – Doppler frequency (angle-Doppler) domain. The ideal two-dimensional (2D) filter is shown in Fig. 1 while the practical filter used in this work is shown in Fig. 2. Clearly, the width of the band-stop filter is an important design parameter. However, analysis of the impact of this parameter is beyond the scope of this paper.

The space-time data, **x**, *and space-time steering vector* are filtered using the band-stop filter coefficients.

$$\hat{\mathbf{X}} = \mathbf{W} * \mathbf{X}, \quad (6)$$

$$\hat{\mathbf{S}} = \mathbf{W} * \mathbf{S}, \quad (7)$$

where **X** and **S** represent the space-time data and steering vector arranged as $M \times N$ matrices, * 2D convolution and the hat (^) above a variable represents filtered data. The new transformation matrix is then given by

$$\hat{\mathbf{T}} = \left[\hat{\mathbf{s}}(f_{-1},\theta_{-1})\ \ \hat{\mathbf{s}}(f_{-1},\theta_0)\ \hat{\mathbf{s}}(f_{-1},\theta_1)\ \hat{\mathbf{s}}(f_0,\theta_{-1})\right.$$
$$\left.\hat{\mathbf{s}}(f_0,\theta_0)\ \hat{\mathbf{s}}(f_0,\theta_1)\ \ \hat{\mathbf{s}}(f_1,\theta_{-1})\ \ \hat{\mathbf{s}}(f_1,\theta_0)\ \ \hat{\mathbf{s}}(f_1,\theta_1)\ \right]. \quad (8)$$

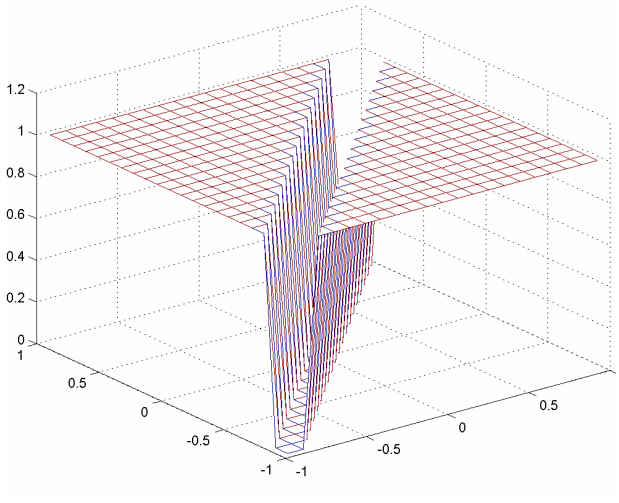

Figure 1: Ideal Two Dimensional Bandstop Filter

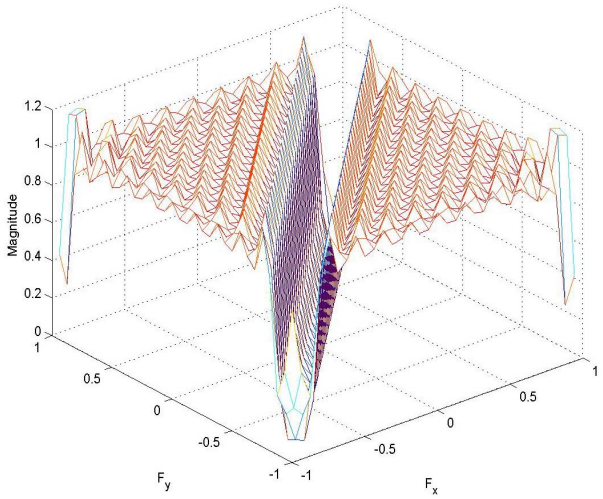

Figure 2: Bandstop filter used in pre-filtering process

The JDL adaptive process continues using Eqns. (2)-(4) with the filtered data $\tilde{\mathbf{x}}$ replacing the original space-time data **x** and the filtered steering vector $\tilde{\mathbf{s}}$ replacing the original space-time steering vector **s**. Note that incorporating the filter is made possible only using the transformation matrix introduced in [3].

3. *NUMERICAL EXAMPLES*

This section presents numerical results illustrating the gains due of the pre-filtering scheme described in Section 2.

3.1 *Simulated Data*

The first example uses $N = 12$, $M = 14$ and a filter size of 21×21. The filter is designed to approximate the ideal filter in Figure 1. Figure 2 plots the frequency response of the filter used in this example. Table 1 lists the parameters of the

antenna array and interference used in this example. The table also lists the parameters used in the processing.

Figure 3 plots the angle-Doppler response of the data within the target range bin. The clutter ridge, with slope 1, is clearly seen. The target amplitude is artificially enhanced to be visible.

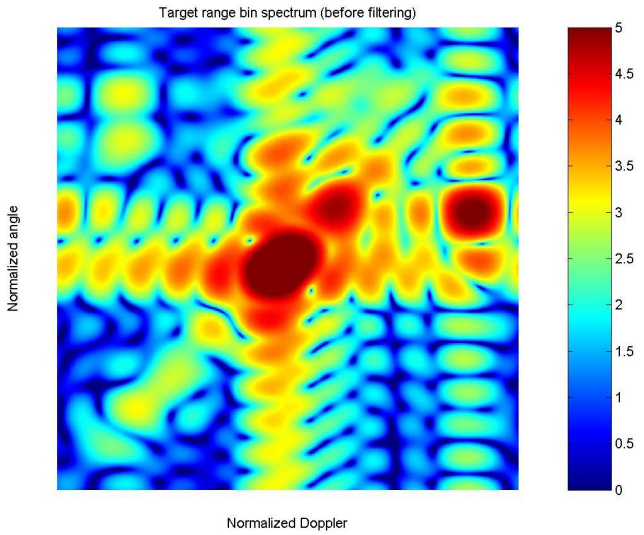

Figure 3 : Angle-Doppler clutter ridge before filtering

Figure 4 plots the angle-Doppler response of the post-filtered data within the target range bin. The clutter ridge is clearly eliminated. Note that due to the type of filter used, the target information does not appear corrupted. However, by accounting for the change in the steering vector using Eqn. (7), any impact of the filter on the target is accounted for. This accounting for the change in steering vector is also taken into account in the JDL algorithm in Eqn. (3).

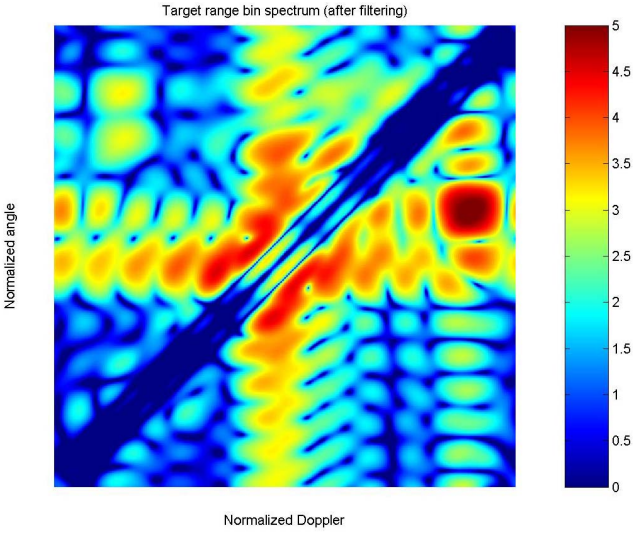

Figure 4: Angle-Doppler clutter ridge after filtering

Table 1: Parameters for example using simulated data

Number of Pulses	14
Number of Elements in Array	12
Element Spacing	0.5 λ
Pulse Repetition Frequency	1024 Hz
Transmit Array Weighting	Uniform
Number of Clutter Patches	181
Target Signal-to-Noise Ratio (per element-pulse)	0dB
Normalized Target Spatial Freq	0.1
Target Normalized Doppler	0.4
Thermal Noise Power	Unity
Clutter-to-Noise Ratio	50dB
Number of Doppler bins in LPR	3
Spacing between Doppler Bins (normalized frequency)	0.05
Number of Angle Bins in LPR	3
Spacing between Angle Bins (normalized frequency)	0.05
Number of Filter Weights in Spatial Dimension	21
Number of Filter Weights in Time Dimension	21
Normalized Filter Notch Width (in Angle-Doppler space)	0.14

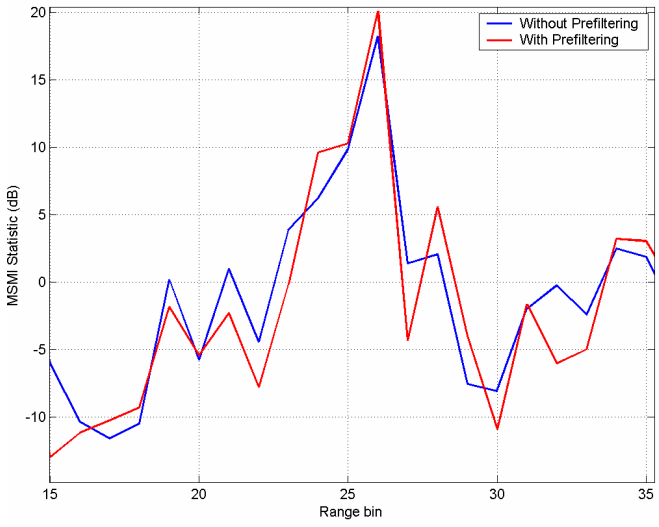

Figure 5: Impact of pre-filtering with simulated data

Figure 5 plots the MSMI statistic versus range bin using JDL with and without pre-filtering. Figures 1 and 2 illustrate the ideal and practical filters used to suppress the clutter ridge. A weak target (0dB) is inserted in range bin 26. Note

the improved discrimination between the target and surrounding range bins, an improvement of approximately 1.5dB. It is important to emphasize that this gain is achieved purely due to pre-filtering the clutter. The elimination of the clutter before translating the data to angle-Doppler space implies a lower interference level in angle-Doppler space, allowing for improved performance. The next example illustrates the performance improvements in measured data.

3.2 *MCARM Data*

This example illustrates the impact of pre-filtering the clutter when using measured data from the Multi-Channel Airborne Measurements (MCARM) program [5]. The MCARM database includes a vast collection of clutter and signal measurements collected by an airborne radar over multiple flights with multiple acquisitions on each flight. The acquisitions used in this example uses a N=22 element rectangular array arranged in a 2×11 grid. Each CPI comprises 128 pulses (M=128). Also provided with the data is a set of measured spatial steering vectors for some specified azimuth and elevation angles. This example uses data from acquisition 575 on flight 5, acquisition cycle 'd'.

This example uses an injected target with amplitude chosen such that it cannot be distinguished without adaptive processing. The target is injected at broadside and Doppler bin -9 into range bin 290.

The use of a 2×11 array requires careful filtering of the MCARM data. The notion of the clutter covering a single ridge in angle-Doppler space assumes a linear antenna array. The data, therefore, is filtered in two batches using 11 elements in each batch. Furthermore, the use of measured data implies the standard steering vector (of phase shifts) is not valid and the measured steering vectors must be used in the pre-filtering process. Figure 6 plots the clutter ridge in the MCARM data. The amplitude of the injected is increased by 20dB to be visible in this non-adaptive processing. The clutter ridge is clearly visible.

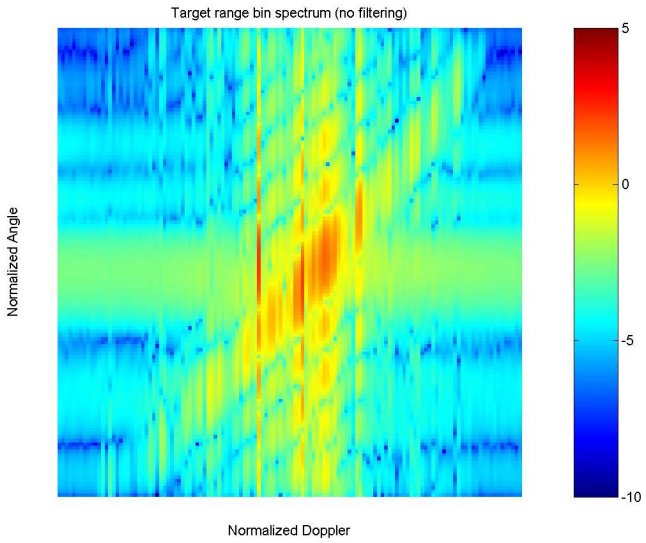

Figure 6: Angle-Doppler clutter ridge before filtering (MCARM Data)

Figure 7 plots the angle-Doppler clutter ridge after using the band-stop filter. The clutter ridge is clearly eliminated without significantly affecting the target. The filter uses 21 coefficients in both the spatial and temporal dimensions.

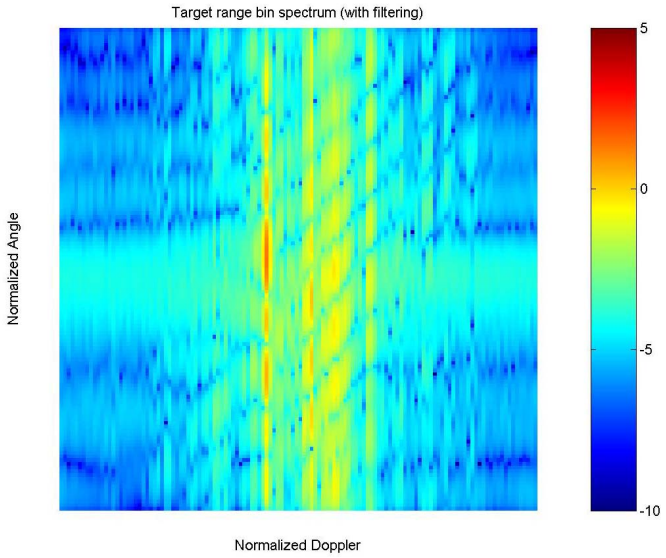

Figure 7: Angle-Doppler clutter ridge after filtering (MCARM Data)

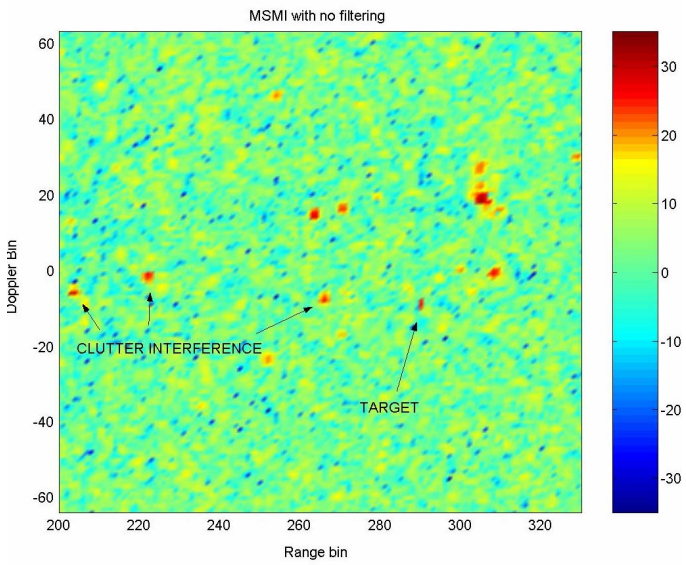

Figure 8: MSMI Statistic versus Doppler and Range (No Pre-Filtering)

Figure 8 plots the modified sample matrix inversion (MSMI) statistic versus Doppler bin and range without any pre-filtering. While the target is visible, false alarms due to the clutter are also visible. Figure 9 plots the MSMI statistic when using the pre-filtered data. As is clear, the false alarm rate due to the clutter has been significantly reduced. The injected target is clearly visible. Note that the other targets visible in this figure were identified earlier as corresponding to highways with vehicles at highway speeds [6].

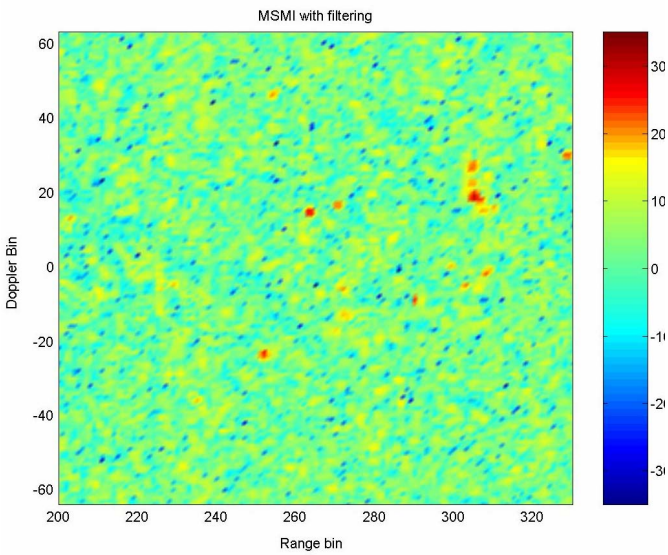

Figure 9: MSMI versus Doppler and Range using pre-filtered data

4. *CONCLUSIONS*

This paper has presented a pre-filtering approach to eliminating the clutter before adaptive processing. The algorithm proposed here uses the fact that the clutter lies, mainly, on a single ridge in angle-Doppler space. Design and use of a two-dimensional band-stop filter eliminates all signals lying along this ridge. Numerical examples using both simulated and measured data illustrate the performance gains available by pre-filtering the clutter.

The approach suggested here is relatively simple and does not require significant additional processing. In this regard, it is hoped that the work here is a first step to more sophisticated algorithms that exploit *a priori* knowledge in the adaptive process.

REFERENCES

1. L. Brenner and I. Reed, "Theory of airborne radar", *IEEE Trans. on Aerospace and Electronic Systems*, vol. 9, 1973, pp. 237-252.

2. J. Ward, "*Space-time adaptive processing for airborne radar*", MIT Lincoln Laboratory Technical Report F19628-95-C-0002, December 1994.

3. H. Wang and L. Cai, "On adaptive spatial-temporal processing for airborne surveillance radar systems", *IEEE Trans. on Aerospace and Electronic Systems*, vol. 30, 1994, pp. 660-669.

4. R.S. Adve, T.B. Hale and M.C. Wicks, ""Joint Domain Localized adaptive processing in homogeneous and non-homogenous Environments. Part I: Homogenous Environments", *IEE Proc. on Radar, Sonar and Navigation,* vol. 147, *(*April) 2000, pp. 57-65.

5. D. Sloper, D. Fenner, J. Arntz, and E. Fogle, "Multi-channel airborne radar measurement (MCARM), MCARMflight test," Contract F30602-92-C-0161, Westinghouse Electronic Systems, April 1996.

6. R.S. Adve, M.C. Wicks, T.B. Hale and P. Antonik, "Ground moving target indication using knowledge based space-time adaptive processing", *Proc. of the 2000 IEEE International Radar Conference*.

BIOGRAPHIES

Raviraj S. Adve was born in Bombay, India on Sept. 11th 1969. He received his B.Tech. from the Indian Institute of Technology, Bombay in 1990 and his Ph.D. from Syracuse University in 1996, both in Electrical Engineering.

From January 1997 to August 2000, Prof. Adve was with Research Associates for Defense Conversion of Marcy, N.Y. working on contract with the Air Force Research Laboratory in Rome N.Y. In August 2000 he joined the Dept. of Electrical and Computer Engineering at the University of Toronto, where he is currently an Assistant Professor.

Prof. Adve is a Senior Member of the IEEE and a member of the Professional Engineers of Ontario. His Ph.D. dissertation received the Syracuse University Doctoral Prize. He also received the APSC Undergraduate Teaching Award in 2003 from the University of Toronto and a Spring 2004 teaching award from the Dept. of Elec. and Comp. Eng.

Prof. Adve can be reached at:

10 King's College Road,
Dept. of Elec. and Comp. Eng.,
University of Toronto,
Toronto, ON M5S 3G4, Canada.